Characterization of an ultrafiltration membrane modified by sorption of branched polyethyleneimine

Aurélie Escoda[a], Boris Lakard[a], Anthony Szymczyk[b], Patrick Fievet[a*]

[a]*Université de Franche-Comté, Institut UTINAM, UMR CNRS 6213, 25030 Besançon cedex, France*
Tel. +33 (3) 81 66 20 32; Fax: +33 (3) 81 66 62 88; email: patrick.fievet@univ-fcomte.fr
[b]*Université de Rennes 1, Chimie et Ingénierie des Procédés, Sciences Chimiques de Rennes, UMR 6226 CNRS, ENSCR,*
263 avenue du Général Leclerc, case 1011, CS 74205, 35042 Rennes cedex, France

ABSTRACT

A polyethersulfone ultrafiltration membrane was functionalized by a cationic polyelectrolyte, the branched polyethyleneimine (BPEI). Several characterization techniques were carried out to investigate the membrane modification. Atomic force microscopy and the tangential streaming potential measurement were used to characterize the outer surface of the membrane. Both techniques indicated that the surface was really modified. Electrokinetic measurements showed a charge reversal of the outer surface of the membrane when the cationic polyelectrolyte adsorbs onto the membrane. This charge reversal (from negative values for the unmodified membrane to positive values for the modified membrane) was also observed with membrane potential measurements. With the help of salt diffusion measurements, it was concluded that the charge reversal observed in membrane potential experiments resulted from the adsorption of BPEI onto the pore walls of the membrane (and not only on the outer surface of the membrane as could be concluded from single tangential electrokinetic measurements).

Keywords: Functionalized membrane; Polyethersulfone; Polyelectrolyte; Streaming potential; Membrane potential

1. Introduction

Currently, applications of membranes have been developed well beyond the exploitation of the membrane separation process in water treatment. For example, membranes are key elements of fuel cells [1], a variety of chemical and biosensors [2], drug deliverable systems with controllable release [3], separation devices based on affinity chromatography [4]. They can also be used as templates in the fabrication of ordered nanometer-sized structures [5], as scaffolds in tissue engineering [6], as membrane microarrays in high-throughput screening technology [7], for the purification of biological fluids or for bio-molecule separation [8], in medical diagnoses [9],after functionalization for decreasing or eliminating of membranes bio(fouling) [10,11].

Such diversity in membrane applications has led to a growing demand for semi-permeable membranes with a molecular structure containing reactive functional groups. Depending on a specific application, these reactive moieties play various roles such as binding sites for immo-bilization, participation in ion exchange, conformational changes in a stimuli response. More, the efficiency of the membranes depends on its molecular and structural architecture (i.e. functional groups distribution: 2-D or 3-D distribution, uniformity), shielding of functional groups and their accessibility or membrane morphology.

Amongst the various techniques allowing the chemical functionalization of a membrane by reactive functional groups, the sorption of polyelectrolyte nanolayers on a membrane surface is one of the most promising. Indeed, nano-assembly of polyelectrolytes is a simple, versatile and environmental benign technique for making layered polymeric coatings [12], which could also be used to

*Corresponding author.

prepare separation membranes. Because of the high hydrophilicity of polyelectrolytes, the membranes so obtained are expected to be appropriate for solvent dehydration. By depositing either one polycation or polyanion layer or by depositing alternately a polycation and a polyanion on an initially charged membrane, an ultrathin and chemically well-defined polyelectrolyte film can be obtained. In general, a layer of polyelectrolyte has a uniform thickness of 0.5–3 nm [12]. This thickness can be affected by such deposition conditions as concentration and pH of the polyelectrolyte solution, ionic strength, and temperature. During the past few years, polyelectrolyte films have attracted significant attention as a potential membrane for separation applications. For example, polyelectrolyte membranes have been used for liquid separations by pervaporation, and these membranes were found to be highly selective to water permeation [13–15].

The aim of this work is to investigate the surface charge properties of an ultrafiltration membrane that has been functionalized by a cationic polyelectrolyte, the branched polyethyleneimine (BPEI). Tangential and transversal techniques are used to characterize the surface charge properties of both the outer surface of the membrane and the pore walls.

2. Experimental

2.1. Membranes and chemicals

PES (polyethersulfone) membranes (Rayflow®-IRIS membrane) manufactured by Novasep (France) with a cut-off of 100 kg mol^{-1} were used. They were supplied as flat sheets stored in glycerin.

Before being functionalized by cationic branched-polyethyleneimine (BPEI, molar mass ~30 000 g mol^{-1}), membranes were cleaned by immersion in NaOH 2 M during 2 h and then immersed in milli-Q quality water (conductivity <1 μS cm^{-1}) during 8 h. The BPEI was purchased from Sigma-Aldrich. BPEI used in this work contains ca. 25% of tertiary amine groups, 50% of secondary amine groups and 25% primary amine groups [16]. BPEI solutions were freshly prepared by direct dissolution in milli-Q quality water. The final BPEI concentration was of 10 mg/ml. The membranes were functionalized by immersion in BPEI solutions during 18 h at room temperature. The protonation of BPEI is rather easy due to its relatively strong base character: the BPEI protonation is already few per cents at a pH value higher than 9 [17]. It appeared to be sufficient at a pH value of 8 for a strong BPEI anchoring on all the studied membranes. The BPEI immobilization on membranes was clearly evidenced by dye staining [18]. When the PES membrane, negatively charged, is immersed in the cationic BPEI, the cationic polymer chains are electrostatically attracted by the

negative charges covering the membrane surface. Thus, PES membrane counter-ions, initially, are substituted by cationic polymer chains, transported by diffusion near the membrane, and a surface ion pairing occurs between polymer chains and PES negative charges. Consequently, the mechanism of deposition is based on the substitution of the PES membrane counter-ions by charged polyelectrolyte. This fixation is possible thanks to the electrostatic affinity between the cationic BPEI and the negatively charged membrane surface.

The electrolytes (KCl, LiCl and MgCl$_2$) used for the characterization of membranes were of pure analytical grade (PROLABO) and solutions were prepared from milli-Q quality water (conductivity <1 μS cm^{-1}).

2.2. Atomic force microscopy (AFM)

AFM was used to visualize the surface structures of both initial and modified membranes and to determine their surface rugosities. The AFM instrument used in the present study was a PicoSPM, a commercial device from Molecular Imaging (USA). Cantilevers used were gold-coated Si$_3$N$_4$ tip (200 μm-long triangular cantilever and 0.1 N/m force constant). Contact imaging mode in air was selected to study the membranes at room temperature (20±3°C). All the membrane samples were imaged without preparative procedure so as not to affect their structure. Images were obtained over an area of 5×5 μm^2 for initial and modified membranes. Once a clear image was obtained, the mean surface roughness was determined by the help of surface analysis software associated with PicoSPM.

2.3. Tangential streaming potential measurements

Streaming potential is probably the most widely used technique for the characterization of electrical properties of membrane/solution interfaces [19–28]. In the present study, streaming potential measurements were performed by applying a pressure gradient along the outer surface of the membrane (tangential streaming potential) [22–28]. Experiments were conducted with a ZETACAD zetameter (CAD Instrumentation). The apparatus measures the streaming potential resulting from the pressure-driven flow of an electrolyte solution through a thin slit channel formed by two identical membrane surfaces facing each other. The electrolyte solution was forced through the slit channel using nitrogen gas. The pressure difference between the channel ends was controlled by means of a differential pressure sensor. The streaming potential ($\Delta\phi_s$) developed in the solution along the channel was measured by means of a pair of Ag/AgCl wire electrodes placed at the inlet and outlet of the channel and linked to a Keithley multimeter (model 2000). The streaming

potential was measured for continuously increasing pressure pulses from 0 to ~500 mbar (the solution was pushed using nitrogen gas).

Samples of 75×25 mm (corresponding to the measuring cell dimensions) were cut in sheet membranes. Modified and unmodified samples were soaked overnight in the electrolyte solution in order to equilibrate the membrane surfaces with the measuring solution. The membrane samples were placed further in the measuring cell and tangential streaming potential measurements were carried out at various channel heights by using Teflon spacers of several thicknesses. The length (l) and the width (L) of the channel were 75 and 25 mm, respectively. Measurements were carried out at 20±3°C. A more detailed description of the apparatus can be found elsewhere [27,28].

2.4. Membrane potential and salt diffusion measurements

Another way to access to the charged state of a membrane is to measure the membrane potential since it reflects the partition of ions into the pores [29–34].

The test cell used for the electrochemical measurements is similar to that described elsewhere [33]. It is composed of two polycarbonate half-cells of volume 70 cm^3 and the membrane is clamped between them by using silicone rubber rings. Fluids in both compartments are stirred vigorously, at the same speed, by a magnetic stirrer in order to minimize concentration polarization at the membrane surfaces. The exposed membrane area was of 7.1 cm^2.

Membrane potential measurements were performed by keeping the concentration of the solution at one side of the membrane, C_1, constant ($C_1 = 10^{-3}$ M) and gradually changing the concentration of the solution at the other side, C_2, from 10^{-3} M to 10^{-2} M. For the whole study, the active layer of the membrane was put in contact with the higher concentration solution (C_2). The membrane was left overnight in a solution of concentration C_1 before placing it in the measuring cell.

When a neutral membrane separates two compartments (1 and 2) containing the same electrolyte at different concentrations (C_1 and C_2), the concentration difference acts as a driving force for the diffusion of both cations and anions through the membrane pores. In most electrolytes, cations and anions have different diffusion coefficients, which therefore lead to an electric charge flux through pores. Consequently, an electric field arises between pore ends, which accelerates less mobile ions and decelerates the more mobile ones. At steady state, the flux of positive charges equals that of negative charges so that no net electrical current flows through the membrane pores. The resulting electrical potential difference, called diffusion potential ($\Delta\varphi_{diff}$), can be expressed by means of the so-called Planck–Henderson equation:

$$\Delta\varphi_{diff} = -\frac{RT}{F}\left(\frac{t^+}{z^+}+\frac{t^-}{z^-}\right)\ln\left(\frac{C_2}{C_1}\right) \qquad (1)$$

where C_2 is assumed to be greater than C_1, t^+ and t^- are transport numbers of cations and anions in bulk solution, respectively, z^+ and z^- are their charge numbers, respectively, R is the ideal gas constant, T the absolute temperature and F the Faraday constant.

For the case of charged membranes, the membrane potential can be viewed as a modified diffusion potential accounting for the effect of the membrane fixed charge on ion transport inside pores. Thus, for charged membranes, the membrane potential takes the following form:

$$\Delta\varphi_m = -\frac{RT}{F}\left(\frac{t_m^+}{z^+}+\frac{t_m^-}{z^-}\right)\ln\left(\frac{C_2}{C_1}\right) = \frac{RT}{F}\left(1-2t_m^+\right)\ln\left(\frac{C_2}{C_1}\right) \qquad (2)$$

where t_m^+ and t_m^- are the apparent transport numbers of cations and anions, respectively, in the membrane pores ($t_m^+ + t_m^- = 1$).

As shown by Eq. (2), apparent ion transport numbers can be determined from the slope of the plot of $\Delta\varphi_m$ vs. $\ln(C_2/C_1)$.

According to Eqs. (1) and (2), the membrane potential will be higher (lower) than the diffusion potential for a membrane with a positive (negative) fixed charge. The sign of the membrane charge can then be deduced from the membrane potential value.

The membrane potential ($\Delta\varphi_m$) is defined as the difference between the potential in bulk solution of higher concentration and the potential in bulk solution of lower concentration. It was calculated by subtracting the concentration potential (resulting from different concentrations of solutions) from the cell potential ($\Delta\varphi_{cell}$) measured by inserting two Ag/AgCl electrodes (connected to a voltameter) directly into the bulk solutions:

$$\Delta\varphi_m = \Delta\varphi_{cell} - \frac{RT}{F}\ln\left(\frac{C_1}{C_2}\right) \qquad (3)$$

The electrode inserted into solution of lower concentration was grounded. In order to cancel the effect of the asymmetry potential, the electrodes were interchanged in the two compartments and the average of the two measurements was taken for $\Delta\varphi_{cell}$ [34]. The asymmetry potential was not greater than 0.2 mV.

It should be noted that Eqs. (1)–(3) are valid for diluted solutions because concentrations were used instead of activities.

In salt diffusion experiments, one compartment of the cell was filled with an electrolyte solution ($C_2 = 0.5$ M) and the other with milli-Q quality water. The conductivity of the fluid inside the diffusate compartment was monitored as a function of time with a Tacussel XE 100 conductivity cell electrode connected to a Tacussel CDRV 62 conductimeter. During the experiment, the temperature was controlled in both compartments in order to ensure that its variation was negligible ($\Delta T \leq \pm 1\,^{\circ}$C). Indeed, the transfer of the electrolyte through the membrane must occur in the absence of any temperature gradient. Moreover, the electrolyte conductivity is sensitive to temperature fluctuations. During the experiment, the amount of electrolyte transferred from the feed compartment to the diffusate compartment was quite negligible as compared with the initial amount in the feed compartment so that the electrolyte concentration inside the feed compartment (C_2) was considered constant. The membrane was soaked overnight in a solution of concentration C_2 before starting salt diffusion experiments.

Salt permeability through a membrane, P_s, can be determined from salt diffusion measurements by means of Fick's first law for a quasi-steady state. The solute flux, J_s, through a membrane can be written as:

$$J_s = \frac{V_1}{A_m}\frac{dC_1}{dt} = P_s \left[C_2 - C_1(t)\right] \tag{4}$$

where A_m is the membrane area in contact with solutions, V_1 the volume of the solution in the diffusate compartment, C_1 and C_2 the electrolyte concentrations inside the diffusate compartment and the feed compartment, respectively.

After substitution of concentrations by electrolyte conductivities, the integration of Eq. (4) with time leads to the following equation:

$$\lambda_1(t) = \left(\frac{A_m}{V_1}\lambda_2 P_s\right)t + \lambda_w \tag{5}$$

where λ_1 and λ_2 are the conductivities of solutions in the diffusate and feed compartments, respectively, and λ_w the conductivity of milli-Q quality water.

3. Results and discussion

3.1. AFM images of membranes

The mean surface roughness of the PES membrane was estimated at 42.5 nm by analysis of its AFM image. After immersion in the polyelectrolyte solution during 18 hours, the surface roughness of the BPEI-modified membrane was estimated at 17.8 nm (Fig. 1). Consequently, the surface roughness decreases by a factor of ~2.5 when a BPEI film is coated onto the membrane surface. We can also observe that the roughness values deduced from the AFM images are coherent with the values obtained in previous studies [35,36].

3.2. Zeta potential of membranes

Fig. 2 gives an example of tangential streaming potential measurements carried out with modified (PES+BPEI) and unmodified (PES) membranes in 10^{-3} M KCl solution at pH = 5.8. As can be seen, a good linearity is obtained for both membranes. The streaming potential coefficient of each membrane can be deduced from the slope of the plot of $\Delta\varphi_s$ versus ΔP. The results clearly show that the charge at the outer surface of the membrane is reversed upon sorption of the cationic BPEI. A low negative charge is measured with the unmodified membrane despite the fact that there are no ionizable functional groups on polyethersulfone chains. To explain the charge behavior of non-ionogenic surfaces, it is usually postulated that a preferential adsorption of anions (chloride ions here) occurs, anions being less hydrated than cations. It was also suggested that chemical post-treatment of membrane materials could be responsible for the observed surface charge of this kind of surfaces [37].

Due to the porous structure of UF membranes, cares must be taken to convert tangential streaming potential experimental data into zeta potential. Indeed, in the conventional electrokinetic theory, it is assumed that both streaming and conduction currents involved in the streaming potential process flow through an identical path. This assumption does not hold anymore when streaming potential measurements are performed with porous substrates. Indeed, in such a case the streaming current flows only through the channel whereas the conduction current is expected to flow wherever the electric conductivity differs from zero, i.e. through both the channel and the membrane pores filled with electrolyte solution. The relation between the streaming potential across channels whose walls are formed by porous substrates and the zeta potential (ζ) has been established by Yaroshchuk and Ribitsch [38]. For rectangular slit channels, the relation takes the following form:

$$\left(\frac{\Delta P}{\Delta\varphi_s}\right)_{I=0} = \frac{\eta\,\lambda_0}{\varepsilon_0\,\varepsilon_r\,\zeta} + \frac{2\,\eta\,h_m\,\lambda_m}{\varepsilon_0\,\varepsilon_r\,\zeta}\left(\frac{1}{2h}\right) \tag{6}$$

where I is the electric current, λ_0 is the bulk channel conductivity, ε_0 is the vacuum permittivity, ε_r is the relative dielectric constant of the solvent, h_m is the effective thickness in which the conduction current flows inside the

(a)
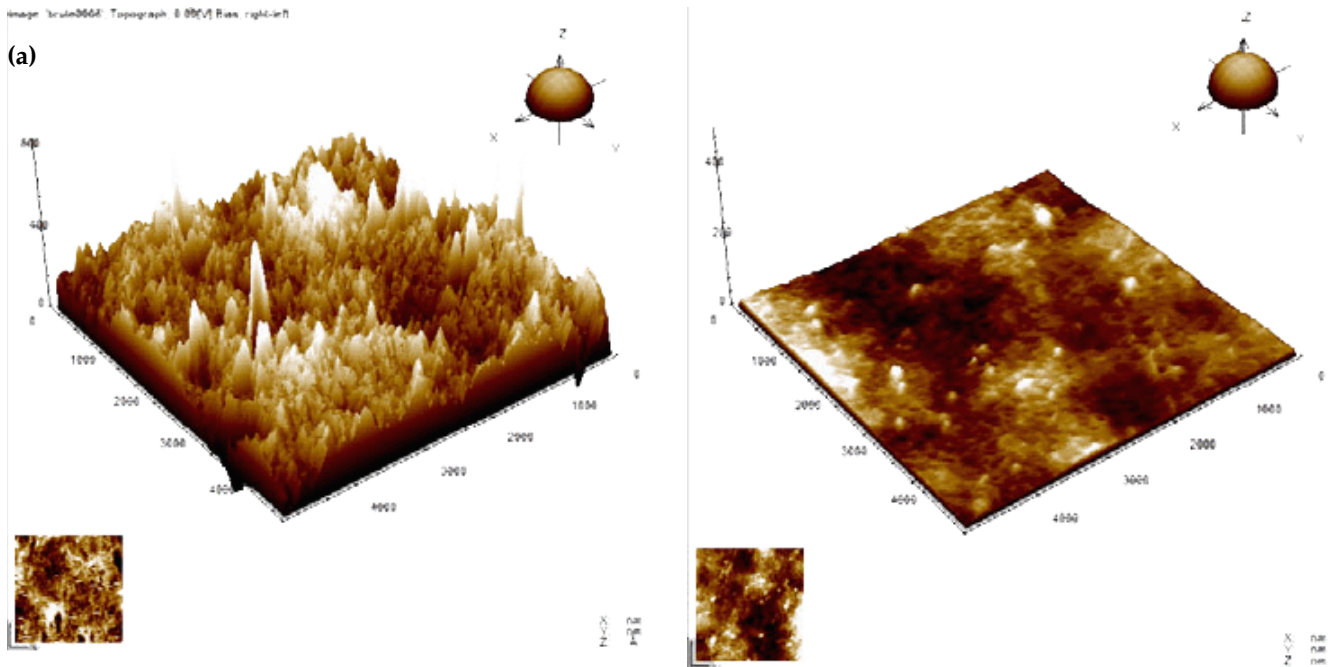
Fig. 1. AFM images of (a) PES and (b) PES+BPEI membranes. Contact mode, scan size is 5×5 µm^2.
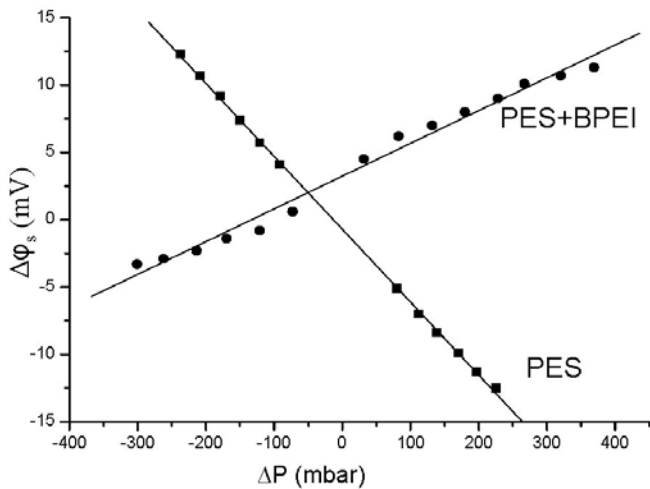
Fig. 2. Tangential streaming potential ($\Delta\varphi_s$) vs. applied pressure difference (ΔP); 10^{-3} M KCl, pH = 5.8. 2 h = 90 µm.

Fig. 3. Reciprocal streaming potential coefficient (SP^{-1}) vs. reciprocal channel height (1/2 h) for the PES+BPEI membrane; 10^{-3} M KCl, pH = 5.8.

membrane pores and λ_m is the electric conductivity inside the membrane pores.

According to Eq. (6), the reciprocal streaming potential coefficient ($\Delta P/\Delta\varphi_S$) is expected to vary linearly with the reciprocal channel height (1/2 h). Consequently, streaming potential measurements carried out at different channel heights should allows the determination of the correct value of the zeta potential by extrapolating the regressed line $\Delta P/\Delta\varphi_s = f(1/2 h)$ at infinitely large channel heights.

Fig. 3 shows that a linear relation between the reciprocal streaming potential coefficient and the reciprocal

channel height is obtained as predicted by Eq. (6) for the modified membrane. From the intercept at infinite channel height, a zeta potential of +14.9 mV is estimated.

The stability of the modified membrane was also investigated by performing streaming potential measurements in 10^{-3} M KCl solution over a period of 21 days. Between two measurements, the membrane was left in 10^{-3} M KCl solution which was changed every day. The results obtained clearly show that the BPEI film is stable during at least 3 weeks in this solution (Fig. 4).

3.3. Membrane potential measurements

Fig. 5 presents the variation of the membrane potential versus the logarithm of concentration ratio (i.e. ln (C_2/C_1),
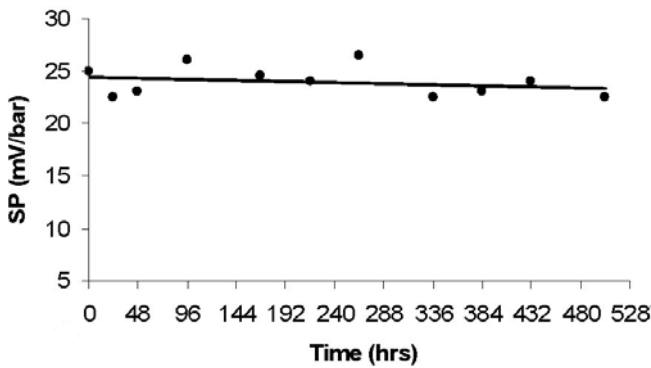
Fig. 4. Streaming potential coefficient (SP) vs. time for the PES+BPEI membrane; 10^{-3} M KCl, pH = 5.8. $2\,h$ = 90 μm.

the concentration in compartment 1 being kept constant at 10^{-3} M) for both modified and unmodified membranes.

In Fig. 5, KCl solutions were used for membrane potential experiments. In the particular case of KCl, the diffusion potential is virtually zero since chloride and potassium ions have very close diffusion coefficients (2.03 10^{-9} m^2 s^{-1} and 1.96×10^{-9} m^2 s^{-1}, respectively). Consequently, the sign of membrane potential measured with KCl solutions directly yields the sign of the membrane fixed charge. Results in Fig. 5 clearly show the charge reversal when the negatively charged PES membrane is modified by the BPEI.

The membrane potential is found to vary linearly with the logarithm of concentration ratio for both modified and unmodified membranes. According to Eq. (2), this finding indicates that transport numbers of ions inside the membrane pores are independent of the electrolyte concentration (in the concentration range under investigation). The value of the transport number of potassium ions inside the membrane pores can be deduced from the slope of the straight lines shown in Fig. 5 by means of Eq. (2). For the (unmodified) PES membrane, the cation transport number inside pores is found to be close to 0.57. This value is higher than the transport number of potassium ions in bulk solution (i.e. 0.49 for a KCl solution). This result is in agreement with the negative charge of the PES membrane since potassium ions are in excess within pores with respect to chloride ions (which are coions of the negatively charged PES membrane). When the PES membrane is modified by the BPEI, the membrane charge is reversed. It leads to a decrease in the transport number of potassium ions inside pores, which becomes lower (around 0.30) than its bulk value (i.e. 0.49).

The modified membrane can be described as a multi-layer system that consists of two distinct layers (namely the PES membrane and the BPEI top layer). When applied to multilayer systems, transversal techniques like membrane potential measurement provide a global signal that results from the contribution of all layers. The relative
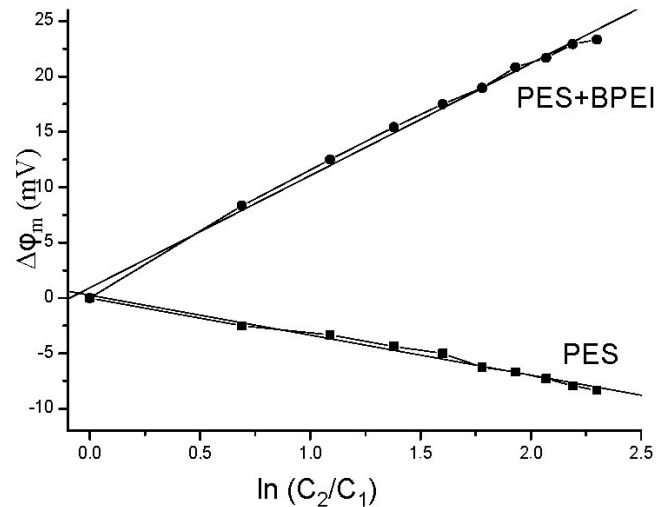
Fig. 5. Membrane potential ($\Delta\varphi_m$) vs. ln (C_2/C_1) for PES and PES+BPEI membranes; KCl electrolyte, pH = 5.8, $C_1 = 10^{-3}$ M, $C_2 = 10^{-3}$ to 10^{-2} M.
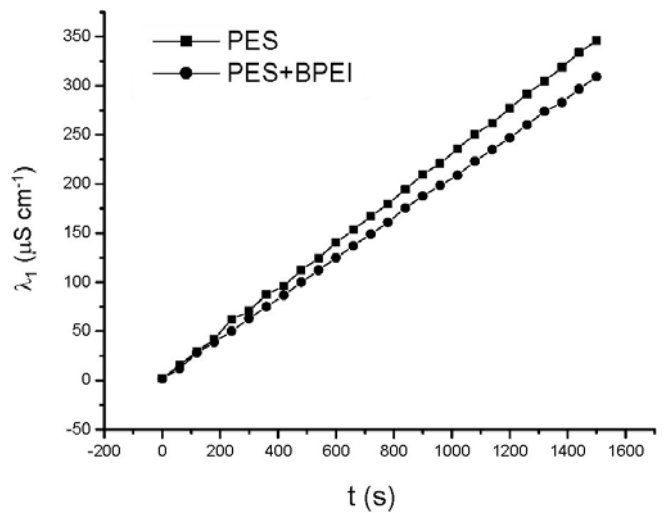
Fig. 6. Variation of the conductivity in the diffusate compartment (λ_1) with time for PES and PES+BPEI membranes; 0.5 M KCl, pH = 6.2.

contribution of each layer to the experimental signal depends on both its structural and electrical properties [39]. In the case of membrane potential, the relative contribution of the various layers depends on their diffusional resistance. According to salt diffusion measurements (see next section), the solute flux for KCl is decreased by only ~10% when the PES membrane is modified by the BPEI. It means that the diffusional resistance of the single BPEI layer does not contribute significantly to the overall resistance to diffusion of the modified membrane. Otherwise stated, the contribution of the BPEI layer does not dominate the overall membrane potential measured through the PES+BPEI membrane.

Table 1
Solute flux (J_s) of KCl, LiCl and MgCl$_2$ electrolytes (0.5 M) for PES and PES+BPEI membranes

Electrolyte	pH	Membrane	Solute flux J_s ($\times 10^{-5}$ mol m^{-2} s^{-1})	Solute flux variation (%)
KCl	5.8	PES	23.13	
		PES+BPEI	20.68	−10.62
LiCl	5.75	PES	15.24	
		PES+BPEI	14.59	−4.31
MgCl$_2$	5.8	PES	13.07	
		PES+BPEI	10.20	−21.95

Since Fig. 5 clearly shows that the membrane fixed charge is reversed when the membrane is modified by the BPEI, our results suggest that the polyelectrolyte did not adsorb only onto the outer surface of the membrane but also onto the pore walls (i.e. within the membrane pores).

3.4. Salt diffusion measurements

Fig. 6 shows the variation of the conductivity in the diffusate compartment with time due to the diffusion of potassium chloride through pores of both modified and unmodified membranes. As expected from Eq. (4), the conductivity (and so the electrolyte concentration) in the diffusate compartment increases linearly with time. The salt permeability (P_s) can then be inferred from the slope of the straight lines (data are collected in Table 1). A slight decrease (around 10%) in the salt permeability is observed with the modified membrane. This means that the diffusional resistance of the BPEI layer is small with respect to that of the PES membrane (this can be explained by the small thickness of the polyelectrolyte layer with respect to that of the underlying PES membrane. Salt diffusion experiments have been carried out with LiCl and MgCl$_2$ as well. Salt permeabilities for the various salts are collected in Table 1. For the unmodified membrane, the sequence of salt permeability is MgCl$_2$ < LiCl < KCl. These results cannot be explained by electrostatic interactions between solutes and the membrane fixed charge (probably because the pore size is not small enough) since this latter is negative for the PES membrane. However, the experimental sequence can be correlated to hydration of the various cations. Indeed, the hydration energy follows the order Mg^{2+} > Li$^+$ > K$^+$. The same sequence of salt permeability is obtained with the modified membrane. The decrease in permeability is much greater for MgCl$_2$ (around 22%) than for KCl and LiCl (around 10% and 4%, respectively). It may result from electrostatic interaction between divalent cations and the positive fixed charge of the BPEI (which adsorbs both on the outer surface of the membrane and inside the PES membrane pores as discussed in the previous section).

4. Conclusions

In this work a polyethersulfone ultrafiltration membrane was modified by sorption of a cationic polyelectrolyte, the branched polyethyleneimine (BPEI). The aim of this study was (1) to give evidence of the modification of the membrane charge after the polyelectrolyte adsorption, and (2) to determine whether the membrane was functionalized only on its outer surface or inside its porous structure as well. Both modified and unmodified membranes were characterized in terms of zeta potential and transport number of cations inside pores (by means of tangential streaming potential and membrane potential measurements, respectively). Tangential streaming potential measurements clearly showed a charge reversal of the outer surface of the membrane. This surface modification is in agreement with AFM analysis carried out with both samples. Membrane potential measurements were carried out through both membranes.

Results showed a charge reversal (from negative to positive) when the polyelectrolyte adsorbs onto the membrane. With the help of salt diffusion measurements, it was concluded that the charge reversal observed in membrane potential experiments resulted from the adsorption of BPEI onto the pore walls of the membrane (and not only on the outer surface of the membrane as could be concluded from single tangential streaming potential measurements).

5. Symbols

A_m — Membrane area, m^2
C — Solute concentration in a compartment, mol m^{-3}
F — Faraday constant, C mol^{-1}
h — Half-height of the slit channel, m
h_m — Thickness of the membrane layer where the conduction current flows, m
I — Electric current, A
J_s — Solute flux, mol m^{-2} s^{-1}
l — Length of the slit channel, m
L — Width of the slit channel, m

P — Hydrostatic pressure, N m^{-2}

P_s — Salt permeability, m s^{-1}

R — Ideal gas constant, $\text{J mol}^{-1}\text{K}^{-1}$

t — Time, s

t_m^+ Apparent transport numbers of cations

t_m^- — Apparent transport numbers of anions

T — Temperature, K

V — Volume of a compartment, m^3

Greek

ε_0 — Vacuum permittivity, $8.854\times10^{-12}\text{ F m}^{-1}$

ε_r — Relative dielectric constant of the solvent

λ_1 — Conductivity of solution in the diffusate compartment, S m^{-1}

λ_2 — Conductivity of solution in the feed compartment, S m^{-1}

λ_w — Water conductivity, S m^{-1}

λ_0 — Conductivity of bulk electrolyte, S m^{-1}

λ_m — Electric conductivity of the membrane, S m^{-1}

η — Viscosity of the electrolyte, $\text{kg m}^{-1}\text{s}^{-1}$

φ — Electrical potential, V

φ_{diff} — Diffusion potential, V

φ_m — Membrane potential, V

φ_s — Streaming potential, V

ζ — Zeta potential, V

References

[1] M.A. Hickner, H. Ghassemi, Y.S. Kim, B.R. Einsla and J.E. McGrath, Chem. Rev., 104 (2004) 4587.

[2] B. Adhikari and S. Majumdar, Progr. Polym. Sci., 29 (2004) 699.

[3] K. Okimoto, A. Ohike, R. Ibuki, O. Aoki, N. Ohnishi, R.A. Rajewski, V.J. Stella, T. Irie and K. Uekama, J. Controlled Release, 60 (1999) 311.

[4] E. Klein, J. Membr. Sci., 179 (2000) 1.

[5] G. Xie, M. Song, K. Mitsuishi and K. Furuya, Appl. Surf. Sci., 241 (2005) 91.

[6] E.E.L. Swan, K.C. Popat and T.A. Desai, Biomaterials, 26 (2005) 1969.

[7] J.X. Tang, N.Y. He, M.J. Tan, Q.G. He and H. Chen, Colloids. Surf. A., 242 (2004) 53.

[8] D.A. Butterfield, Biofunctional Membranes, Plenum Press, New York, 1966.

[9] D.A. Butterfield, D. Bhattacharyya and L. Bachas, J. Membr. Sci., 181 (2001) 29.

[10] T. Knoell, J. Safarik, T. Cormack, R. Riley, S.W. Lin and H. Ridgeway, J. Membr. Sci., 157 (1999) 117.

[11] N. Hilal, V.L. Kochkodan, T. Al-Khatib and T. Levadna, Desalination, 167 (2004) 293.

[12] G. Decher, Science, 277 (1997) 1232.

[13] H. Karakane, M. Tsuyumoto, Y. Meada and Z. Honda, J. Appl. Polym. Sci., 42 (1991) 3229.

[14] K. Richau, H.H. Schwarz, R. Apostel and D. Paul, J. Membr. Sci., 113 (1996) 31.

[15] N. Scharnagl, K.V. Peinemann, A. Wenzlaff, H.H. Schwarz and R.D. Behling, J. Membr. Sci., 113 (1996) 1.

[16] J. Suh, I.S. Scarpa and I.M. Klotz, J. Am. Chem. Soc., 98 (1976) 7060.

[17] J. Suh, S.H. Lee and H.J. Paik, Inorg. Chem., 22 (1994) 33.

[18] Q.T. Nguyen, Z.H. Ping and T. Nguyen, J. Membr. Sci., 213 (2003) 85.

[19] C. Werner, H.J. Jacobasch and G. Reichelt, J. Biomater. Sci., 7 (1995) 61.

[20] K.J. Kim, A.G. Fane, M. Nyström, A. Pihlajamaki, W.R. Bowen and H. Mukhtar, J. Membr. Sci., 116 (1996) 149.

[21] M. Pontié, X. Chasseray, D. Lemordant and J.M. Laine, J. Membr. Sci., 129 (1997) 125.

[22] C. Lettmann, D. Möckel and E. Staude, J. Membr. Sci., 145 (1999) 243.

[23] W.Y. Wang and Y. Ku, J. Membr. Sci., 282 (2006) 342.

[24] C. Werner, H. Körber, R. Zimmermman, S. Dukhin and H.J. Jacobasch, J. Coll. Interf. Sci., 208 (1998) 329.

[25] M. Zembala and Z. Adamczyk, Langmuir, 16 (2000) 1593.

[26] M.J. Ariza and J. Benavente, J. Membr. Sci., 190 (2001) 119.

[27] M. Sbaï, A. Szymczyk, P. Fievet, A. Sorin, A. Vidonne, S. Pellet-Rostaing, A. Favre-Reguillon and M. Lemaire, Langmuir, 19 (2003) 8867.

[28] P. Fievet, M. Sbaï, A. Szymczyk and A. Vidonne, J. Membr. Sci., 226 (2003) 227.

[29] G. Alberti, C. Bastioli, M. Casciola and F. Marmottini, J. Membr. Sci., 16 (1983) 121.

[30] Y. Kimura, H.J. Lim and T. Iijima, J. Membr. Sci., 18 (1984) 285.

[31] A. Yamauchi, M. Shinoda and Y. Hirata, Desalination, 71 (1989) 277.

[32] K. Asaka, J. Membr. Sci., 52 (1990) 57.

[33] A. Szymczyk, P. Fievet, J.C. Reggiani and J. Pagetti, J. Membr. Sci., 146 (1998) 277.

[34] R. Tagaki and M. Nakagaki, J. Membr. Sci., 53 (1990) 19.

[35] M. Pontié, H. Essis-Tomé, A. Elana, Q. Trong and A. Nguyen, C.R. Chimie, 8 (2005) 1135.

[36] N. Hilal, T. Al-Khatib, H. Al-Zoubi and R. Nigmatullin, Desalination, 184 (2005) 45.

[37] A.E. Childress and M. Elimelech, J. Membr. Sci., 119 (1996) 253.

[38] A.E. Yaroshchuk and V. Ribitsch, Langmuir, 18 (2002) 2036.

[39] C. Labbez, P. Fievet, A. Szymczyk, B. Aoubiza, A. Vidonne and J. Pagetti, J. Membr. Sci., 184 (2001) 79.